The Aeronautical Journal (2026), **130**, pp. 1920–1943
doi:10.1017/aer.2026.10147

RESEARCH ARTICLE

Impact analysis of solar cells on fixed-wing UAV: simulation-based performance evaluation under varying environmental conditions

M. S. Gencag[1,2], F. Yildirim Dalkiran[3], E. T. Kekec[2] and M. Konar[3]

[1]Graduate School of Natural and Applied Science, Aeronautical Electrical and Electronics, Erciyes University, Kayseri, Turkiye
[2]Cappadocia Vocational School, Cappadocia University, Nevsehir, Turkiye
[3]Faculty of Aeronautics and Astronautics, Aeronautical Electrical and Electronics, Erciyes University, Kayseri, Turkiye
Corresponding author: M. S. Gencag; Email: samet.gencag@kapadokya.edu.tr

Received: 24 June 2025; **Revised:** 3 February 2026; **Accepted:** 4 February 2026

Keywords: flight endurance; renewable energy in aviation; solar-powered UAV

Abstract

The demand for renewable energy is increasing rapidly due to the need for environmental sustainability and the reduction of energy costs. Solar energy, with its high potential and minimal environmental impact, has become a key energy source, particularly in innovative applications such as unmanned aerial vehicles (UAVs). The integration of solar cells into fixed-wing UAVs enables extended flight durations and enhances operational efficiency, making them a viable solution for long-endurance missions. In this study, the effects on flight performance, energy consumption and battery management of a fixed wing UAV equipped with solar cells are investigated. Two UAV models with the same aerodynamic characteristics, one with solar cells and the other powered only by the battery, are comparatively analysed. Using a simulation model, the effects of solar irradiation, temperature and environmental factors on the energy management of the UAV were evaluated. The findings indicate that the solar-powered UAV has the capability to sustain uninterrupted 24-hour flight by recharging its battery during daylight hours, whereas the battery-only model is restricted to approximately 14 hours of flight time. In the solar-powered model, dynamic altitude management strategies were employed to extend flight duration, utilising excess energy to determine optimal operational scenarios. Furthermore, the integration of solar cells was found to optimise battery consumption, thereby enabling more sustainable flight operations. These results demonstrate that solar-powered fixed-wing UAVs offer significant advantages for long duration missions and present an efficient solution for energy management.

Nomenclature

UAV	unmanned aerial vehicle
SUAV	solar-powered unmanned aerial vehicle
PV	photovoltaic
FCU	flight control unit
SoC	state of charge
GHI	Global Horizontal Irradiance
DNI	Direct Normal Irradiance
DHI	Diffuse Horizontal Irradiance
AM	air mass
BMS	battery management system
MPPT	maximum power point tracking
DC/DC	direct current to direct current
PVC	polyvinyl chloride
I	current
V	voltage

© The Author(s), 2026. Published by Cambridge University Press on behalf of Royal Aeronautical Society.

https://doi.org/10.1017/aer.2026.10147 Published online by Cambridge University Press

Li-ion	lithium-ion
Wh	watt-hour
W/m^2	watts per square meter
°C	degrees Celsius
G_{sc}	solar constant
G_{on}	degrees Celsius
G_{cb}	beam radiation
k	attenuation coefficient
e	Euler's number
I_O	hourly radiation
H_o	daily radiation
A	altitude
a	beam radiation model coefficients
r	empirical correction coefficients
I_c	hourly solar irradiance on surface
T_C	calculated temperature
T_I	initial temperature
H_R	relative altitude
T_D	temperature lapse rate
C	capacity of the battery
V_t	total voltage
S	number of series cells
V_n	nominal voltage of a single cell
P	number of parallel cells
E_t	total energy

Greek symbols

δ	declination angle
Ω_s	sunset hour angle
θ_z	zenith angle
n	day of the year
ω	hour angle
τ_b	beam transmittance ratio
τ_d	diffuse transmittance ratio
φ	latitude

1.0. Introduction

The demand for renewable energy sources is rapidly increasing due to both environmental sustainability goals and the need to reduce energy costs. Among renewable energy sources, solar energy stands out due to its high energy potential and minimal environmental impact. The advancement of photovoltaic (PV) technologies has enabled the efficient conversion of solar energy into electricity, expanding its potential applications, including unmanned aerial vehicles (UAVs). With ongoing research and development, solar cells are becoming increasingly efficient, allowing sunlight to be directly converted into electrical energy, further enhancing their viability for innovative energy solutions [1–4].

With advancements in technology in recent years, solar-powered UAVs have been utilised across a wide range of fields. Notable applications include monitoring and spraying for plant health in agriculture, early detection of forest fires, cargo transportation, search and rescue operations, inspection of power lines and bridges, climate change research, monitoring of marine ecosystems, traffic management in smart city applications, as well as security and air quality monitoring. These applications have yielded effective results, demonstrating the versatility and efficiency of solar-powered UAVs [5–8].

This study examines the effects of solar irradiance, temperature and environmental factors on the flight performance and energy management of a fixed-wing UAV equipped with solar cells. Additionally,

https://doi.org/10.1017/aer.2026.10147 Published online by Cambridge University Press

a comparative analysis was conducted with an identical UAV operating without solar cells. The primary objective of this study is to identify optimal operational scenarios for enhancing the energy efficiency of solar-powered UAVs and to assess their role in sustainable energy applications.

Over the past decade, a number of studies have advanced the field of solar-powered UAV, focusing on endurance enhancement and energy autonomy. Oettershagen et al. [9, 10] demonstrated the AtlantikSolar platform, a lightweight hand-launchable UAV capable of multi-day continuous flight through efficient solar–battery energy management, marking a major step toward perpetual flight capability. Building on this foundation, Mateja et al. [11] developed a simulation model for energy autonomy of small solar UAVs, emphasising the importance of coupling aerodynamic performance with environmental factors such as irradiance and temperature. Similarly, Huang et al. proposed a three-dimensional flight path optimisation method for solar UAVs to maximise solar exposure and minimise power consumption [12], while Lee and Yu integrated gravitational potential energy concepts into path planning for improving endurance [13].

Recent research on solar-powered UAVs has increasingly emphasised the importance of integrated energy management and realistic environmental modeling. For example, Fernandes et al. [14] conducted experimental evaluation of a small fixed-wing UAV equipped with thin-film photovoltaics and high-efficiency power tracking, demonstrating that the solar subsystem was able to sustain most of the cruise demand under favourable conditions.

Similarly, Zhang et al. [15] focused on parameter analysis of solar-powered UAV power systems under non-ideal environmental factors (such as irradiance variation and ambient temperature), highlighting how these external conditions can significantly degrade performance if unaddressed. In another contribution, Gao et al. [16] proposed an energy-management strategy for solar-powered UAVs that combines particle-swarm optimisation of climb and glide phases, demonstrating up to 68% energy savings in the climb stage under realistic mission profiles. However, most of these studies either rely on generalised atmospheric assumptions or neglect the quantitative influence of localised irradiance and temperature variations on mission-level energy balance. The present work addresses this gap by developing a region-specific numerical model for Central Anatolia, Türkiye, incorporating realistic environmental parameters such as irradiance, temperature and cloud cover into the solar–battery interaction framework.

In this study, a fixed-wing solar-powered UAV was developed and modeled to analyse the influence of solar irradiance, ambient temperature and environmental conditions on flight performance and energy management. A dynamic simulation model was established to estimate the energy flow between the solar panels, battery system and propulsion unit under realistic mission profiles. A comparative analysis was conducted between solar-assisted and conventional battery-powered configurations to quantify the improvement in flight endurance and overall energy efficiency.

The novelty of this work lies in the development of an integrated hybrid energy model that couples solar energy input, battery state of charge and aerodynamic performance under realistic weather conditions. Furthermore, the study provides a comprehensive comparative analysis between solar-assisted and conventional UAV configurations, offering quantitative insights into the endurance and energy balance advantages of solar integration. In addition, the UAV and energy system were specifically designed and modeled for the solar and thermal environment of Central Anatolia, Türkiye, thereby contributing region-specific insights into the operation of solar-powered UAVs under mid-latitude conditions.

The remainder of this paper is structured as follows: Section 2 introduces the UAV system and the mathematical modeling framework. Section 3 presents the simulation setup and analysis methodology. Section 4 discusses the results and comparative findings and Section 5 concludes with key insights and directions for future work, including experimental validation efforts.

2.0. Solar energy generation and environmental factors

2.1. Irradiance

Solar irradiance is a fundamental factor in energy generation for PV cells. Solar cells absorb incoming sunlight on their surface and convert it into electrical energy. The performance of PV cells is directly

https://doi.org/10.1017/aer.2026.10147 Published online by Cambridge University Press

dependent on irradiance levels, which are significantly influenced by variables such as geographical location, time of day and seasonal variations [17–19]. Although the Sun generates a constant amount of energy, the rotation of the Earth and its elliptical orbit cause variations in the amount of solar irradiance received at a specific location throughout the day. To determine the amount of energy produced by solar cells, it is essential to calculate the solar irradiance reaching the surface. This calculation is performed using mathematical models and radiation transfer equations that account for the Earth's position relative to the Sun [17, 20–22]. To calculate the solar energy received at a specific location, equations that incorporate the angular position of the Earth relative to the Sun are used. Declination (δ) is defined as the angle between the line directed toward the Sun and the equatorial plane [11]

$$\delta = 23.45 \times \sin\left(\frac{360}{365} \times (284 + n)\right) \tag{1}$$

where n represents the day of the year. The declination angle varies between (-23.45°) and ($+23.45^{\circ}$), reaching its maximum positive value during the summer solstice and its minimum negative value during the winter solstice. Declination remains the same for all locations on Earth and serves as a fundamental parameter in solar irradiance calculations. The hour angle (ω) is an angular measure that represents the position of the Sun relative to the observer's local meridian, changing approximately 15° per hour [11]. It takes negative values before solar noon and positive values after solar noon. Solar time, which is used in hour angle calculations, differs from local time as it is based on the moment when the Sun reaches its highest point in the sky at a given location. This time system is determined by the apparent daily motion of the Sun. The hour angle can be calculated using Equation (2).

$$\omega = 15^{o} \times (Solar\ time - 12) \tag{2}$$

The hour angle (ω) ranges from (-180°) to ($+180^{\circ}$), where negative values represent the time before solar noon and positive values correspond to the time after solar noon.

The zenith angle θ_z is the angle between the incoming solar irradiation and a horizontal surface, making it a crucial parameter in determining the angle at which solar irradiance reaches the surface. The representation of the zenith angle is illustrated in Fig. 1. The zenith angle can be expressed using the following equation:

$$\theta_z = \cos(\varphi) \times \cos(\delta) \times \cos(\omega) + \sin(\varphi) \times \sin(\delta) \tag{3}$$

φ represents the latitude and is converted to radians using the expression $\varphi = latitude \times \pi/180$. The zenith angle ($\theta_z$) ranges from 0° to 90°, where $\theta_z = 0^{o}$ indicates that the Sun is directly overhead, and $\theta_z = 90^{o}$ corresponds to sunset or sunrise. The day length(N) can be calculated using the following equation:

$$\mathrm{N} = \frac{2}{15} \times \mathrm{Arccos}(-\tan\varphi \times \tan\delta) \tag{4}$$

when $\theta_z = 0^{o}$ means the Sun is directly overhead at the top of the atmosphere, the solar irradiance reaching the surface (G_{on}) is determined based on the solar constant (G_{sc}) and the specific day of the year (n). It is calculated using the following equation:

$$G_{on} = G_{sc} \times \left[1 + 0.033 \times \cos\frac{360 \times \mathrm{n}}{365}\right] \tag{5}$$

Since the Earth's orbit is elliptical, the distance between the Sun and the Earth varies by approximately 3.3% throughout the year. This variation affects the amount of solar irradiance reaching the Earth, contributing to seasonal differences. The solar constant G_{sc} is considered an average value and is taken as 1367 W/m^2.

https://doi.org/10.1017/aer.2026.10147 Published online by Cambridge University Press

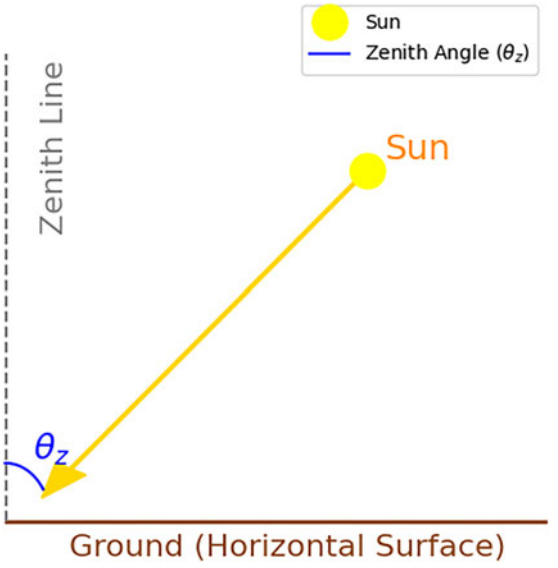


Figure 1. *Illustration of the solar zenith angle.*

The hourly radiation I_o and daily radiation H_o can be calculated using the following equations:

$$I_O = \frac{12 \times 3600}{\Pi} \times G_{sc} \times \left[1 + 0.033 \times cos\frac{360 \times n}{365}\right] \times [cos\,(\varphi) \times \cos\,(\delta) \times (sin\omega_2 - sin\omega_2) \times \frac{\pi \times (w_2 - w_{1)}}{180} \times sin\,(\varphi) \times \sin\,(\delta) \tag{6}$$

ω_2 and ω_1 represent the hour angles corresponding to the selected time intervals. ω_s denotes the solar hour angle at sunrise and sunset, which defines the maximum hour angle, indicating the times when the Sun rises and sets.

$$\mathrm{H_o} = \frac{24 \times 3600}{\pi} \times \mathrm{G_{sc}} \times \left[1 + 0.033 \times \cos\frac{360 \times \mathrm{n}}{365}\right] \times \cos\,(\varphi) \times \cos\,(\delta) \times \sin\omega_s + \frac{\pi \times \omega_s}{180} \times \sin\varphi \times \sin\delta \tag{7}$$

The unit of hourly radiation is expressed as $\frac{J}{m^2}$, while the unit of daily irradiation is $\frac{J}{day \times m^2}$ To convert these values into watt-hours (Wh), appropriate unit conversions are applied.

The air mass (AM) represents the path length that solar irradiation travels through the atmosphere before reaching the Earth's surface and is calculated using the following equation [13, 15]:

$$\mathrm{AM} = \frac{\text{path length travelled}}{\text{vertical depth of the atmosphere}} = \frac{1}{\cos\theta_z} \tag{8}$$

Studies in the literature have developed a method for estimating solar irradiation transmitted under clear atmospheric conditions, considering zenith angle and altitude for standard atmospheric conditions and four different climate types [13, 16]. In solar energy systems, the two most significant types of radiation are beam radiation and diffuse radiation. Beam radiation refers to solar irradiance that reaches the Earth's surface without being scattered by the atmosphere, while diffuse radiation is scattered in multiple directions by the atmosphere, with only a portion reaching the surface [11]. The beam radiation (G_{cb}) can be calculated using the following equation:

$$\mathrm{G_{cb}} = \tau_b \times \mathrm{G_{on}} \times [\cos\,(\varphi) \times \cos\,(\delta) \times \cos\,(\omega) + \sin\,(\varphi) \times \sin\,(\delta)] \tag{9}$$

https://doi.org/10.1017/aer.2026.10147 Published online by Cambridge University Press

where τ_b represents the ratio of transmitted beam radiation to the total radiation incident at the top of the atmosphere. This ratio can be calculated using the following equation:

$$\tau_b = \frac{G_{cb}}{G_o} = a_0 + a_1 \times e^{\left(\frac{-k}{\cos\theta_z}\right)} \tag{10}$$

The hourly solar irradiance reaching the Earth's surface is represented by G_o, while the total solar irradiance incident on the surface at the top of the atmosphere is denoted as G_{on}.

$$G_o = G_{on} \times \cos\theta_z \tag{11}$$

The coefficients a_0, a_1 and k are constants calculated using Equation (12).

$$\begin{aligned} a_0 &= r_0 \times (0.4237 - 0.00821 \times (6 - A)^2) \\ a_1 &= r_1 \times \left(0.5055 - 0.00595 \times (6.5 - A)^2\right) \\ k &= r_k \times \left(0.2711 - 0.01858 \times (2.5 - A)^2\right) \end{aligned} \tag{12}$$

where A represents the altitude of the region above sea level, expressed in meters (m). These equations are valid only when the condition $A < 2.5$ is satisfied. In mid-latitude regions and during summer months, the values of r_0, r_1 and r_k are determined as 0.97, 0.99 and 1.02, respectively [11, 21, 23].

The diffuse solar irradiance (G_{cd}) can be calculated using the following equation:

$$G_{cd} = \tau_d \times G_{on} \times [\cos(\varphi) \times \cos(\delta) \times \cos(\omega) + \sin(\varphi) \times \sin(\delta)] \tag{13}$$

where τ_b, represents the ratio of transmitted diffuse radiation to the total radiation incident at the top of the atmosphere. This ratio can be determined using Equation (14).

$$\tau_d = \frac{G_{cd}}{G_o} = 0.271 - 0.294 \times \tau_b \tag{14}$$

Using the equations above, it is possible to calculate the total irradiance required to determine the energy that can be harvested by solar cells. The total solar irradiance (G_c) reaching a horizontal surface on Earth can be expressed using the following equation.

$$\begin{aligned} G_c &= G_{cb} + G_{cd} = (\tau_b + \tau_d) \times G_{sc} \\ &\times \left[1 + 0.033 \times \cos\frac{360 \times n}{365}\right] \times [\cos(\varphi) \times \cos(\delta) \times \cos(\omega) + \sin(\varphi) \times \sin(\delta)] \end{aligned} \tag{15}$$

The hourly solar irradiance (I_c) reaching a horizontal surface can be expressed using the following equation.

$$\begin{aligned} I_c &= \frac{12 \times 3600}{\pi} \times (\tau_b + \tau_d) \times G_{sc} \times \left[1 + 0.033 \times \cos\frac{360 \times n}{365}\right] \\ &\times \left[\cos(\varphi) \times \cos(\delta) \times (\sin\omega_2 - \sin\omega_1) + \frac{\pi \times (\omega_2 - \omega_1)}{180} \times \sin\varphi \times \sin\delta\right] \end{aligned} \tag{16}$$

A numerical analysis was conducted using these equations. The results of the sample numerical analysis based on these equations are presented in Fig. 2, illustrating the hourly solar irradiance values obtained for the Kayseri region (38.7°N, 35.5°E; elevation $\succ$ 1050 m) in July. Kayseri is located in Central Anatolia, Türkiye, and is characterised by a continental climate with high solar irradiance and low humidity, making it a representative location for evaluating the performance of solar-powered UAV systems.

As solar radiation passes through the atmosphere, it is divided into different components, which are fundamental parameters in the performance analysis of solar energy systems. Solar irradiance consists of three main components: Global Horizontal Irradiance (GHI), Direct Normal Irradiance (DNI) and Diffuse Horizontal Irradiance (DHI). GHI refers to the total solar irradiance received on a horizontal surface and is the sum of DNI and DHI. DNI represents the amount of solar radiation received directly

https://doi.org/10.1017/aer.2026.10147 Published online by Cambridge University Press

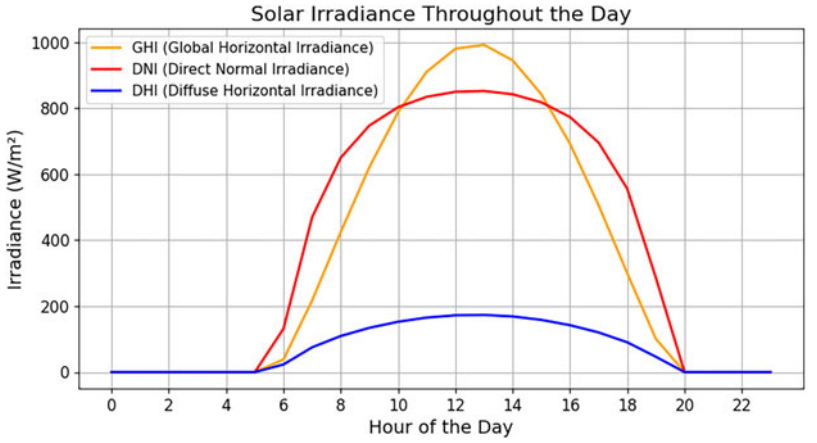


Figure 2. *Hourly variation of Global Horizontal (GHI), Direct Normal (DNI) and Diffuse Horizontal (DHI) solar irradiance throughout a typical July day in the Central Anatolia region, illustrating the diurnal distribution of solar energy components under clear-sky conditions.*

from the Sun without atmospheric scattering. DHI refers to the fraction of solar radiation that is scattered by atmospheric gases, aerosols and clouds, reaching the surface from multiple directions [24].

2.2 Effect of cloudiness

Clouds have a significant effect on solar irradiation, and this effect depends on the type, density and location of the clouds. Clouds block solar irradiation, reducing the energy reaching the surface. This negatively affects the performance of PV systems. In general, clouds can be classified into three main categories. These are high-level clouds (e.g. cirrus), mid-level clouds (e.g. altostratus) and low-level thick clouds (e.g. cumulonimbus). While high-level clouds do not significantly affect irradiation, low-level clouds significantly block solar irradiation, negatively affecting energy production [25–27].

Cloud cover is evaluated using the okta scale, which quantifies the proportion of the sky covered by clouds. This scale ranges from 0 (completely clear sky) to 8 (completely overcast) [28]. The impact of cloud cover on solar irradiance is illustrated in Fig. 3.

In the cloud cover scale, values above 8 oktas are generally associated with a completely overcast sky, where a significant portion of solar irradiance is lost. Studies in the literature indicate that understanding the impact of cloud cover on solar irradiance is crucial for the efficient design and operation of solar energy systems [29–31].

In the simulation model developed for this study, the effect of cloudiness on solar irradiance was explicitly incorporated to ensure realistic environmental modeling. The solar irradiance incident on the PV surface, denoted by I, was adjusted according to the empirical cloud transmittance relationship proposed by Kasten and Czeplak [32], expressed as:

$$I = I_0 \left(1 - 0.75\, X\, cc^{3.4}\right) \tag{17}$$

where I_0 represents the clear-sky global irradiance (i.e. the irradiance in the absence of clouds) and cc denotes the fractional cloud cover, ranging from 0 (completely clear sky) to 1 (fully overcast conditions). This formulation quantifies the attenuation of solar radiation as a function of cloudiness and has been widely adopted in solar energy performance and atmospheric transmittance modeling.

For the numerical simulations in this study, July was selected as the representative month for the Kayseri region because it exhibits the highest average solar irradiance and the lowest mean cloud cover,

https://doi.org/10.1017/aer.2026.10147 Published online by Cambridge University Press

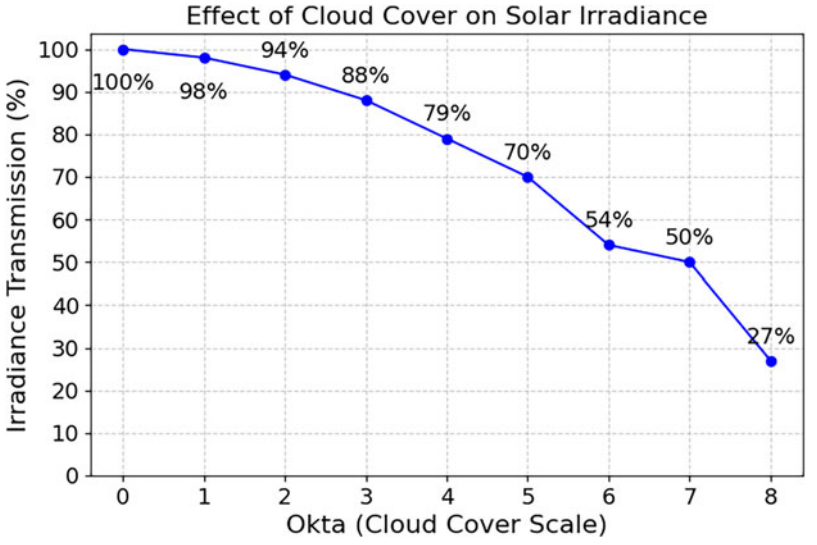


Figure 3. *Effect of cloud cover on solar irradiance transmission.*

providing optimal conditions for evaluating solar-powered UAV performance. According to meteorological data from the Turkish State Meteorological Service (TSMS), the average cloud cover fraction in Kayseri during July ranges between 0.15 and 0.20, corresponding to predominantly clear-sky conditions. Therefore, the inclusion of this cloud attenuation model ensures that the solar energy calculations realistically reflect the influence of atmospheric variability while focusing on the most favourable operational period for solar-powered UAV missions.

2.3 Effect of temperature

Temperature is a critical factor affecting the efficiency of solar cells. As temperature increases, the efficiency of solar cells decreases, negatively impacting the energy conversion process [33]. Each solar cell has a temperature coefficient, which is associated with voltage, current and power parameters, determining the effect of temperature variations on its performance. An increase in temperature degrades the electrical properties of the cells, leading to a reduction in power output and overall efficiency [34, 35].

With every 100-meter increase in altitude, the air temperature decreases by approximately 0,5∼1°C. The distribution of air temperature is largely influenced by latitude, altitude, seasonal variations and topographical features. These temperature drop calculations remain valid up to the tropopause, where the upper atmospheric layer maintains a stable temperature reaching approximately (−51°C). This temperature level is sustained up to an altitude of 20 km [11].

The decline in solar cell efficiency with increasing temperature is primarily related to the heating of the solar cell under solar irradiation and its reduced heat dissipation capacity in high ambient temperatures. Operating PV panels at elevated temperatures not only results in lower electrical power output but also accelerates the degradation process of solar cells, reducing their long-term performance and reliability [36].

The current ambient temperature is correlated with flight altitude and can be calculated using the following equation,

$$T_C = T_I - [H_R\, x\ (T_D\, x\, 100)] \tag{18}$$

where T_C represents the temperature at the flight altitude, T_I is the temperature at ground level, H_R denotes the relative altitude in meters and T_D refers to the temperature lapse rate. According to this calculation, when the relative humidity is below 100%, the temperature decreases by approximately

https://doi.org/10.1017/aer.2026.10147 Published online by Cambridge University Press

1°C per 100 meters of altitude gain. However, when the relative humidity reaches 100%, the release of latent heat due to condensation slows the temperature decline, resulting in a decrease of approximately 0.6°C per 100 meters [37].

Another critical component affected by temperature is lithium-ion (Li-ion) batteries. The sensitivity of Li-ion batteries to temperature variations is a key factor directly influencing their performance. The optimal operating temperature range for Li-ion batteries is between 25°C and 30°C [38]. At low temperatures, the viscosity of the electrolyte increases, leading to a reduction in ionic conductivity and a rise in internal resistance. At (−20°C), in particular, the charge transfer resistance increases significantly, causing a substantial decline in both capacity and power output. Under high temperature conditions, the performance of Li-ion batteries is influenced by more complex mechanisms. Heat generation becomes a significant factor, especially during rapid charging and discharging. Excessive internal temperatures lead to capacity degradation and power loss [39].

2.4 Pollution of air and solar cells

Air pollution and solar cell contamination are two key environmental factors that significantly reduce the efficiency of PV panels. Air pollution weakens solar irradiation as it enters the atmosphere through reflection, scattering and absorption, thereby reducing the amount of sunlight reaching the panels [40]. However, it is very difficult to measure these data precisely due to the continuous variability of environmental conditions. Pollutants such as dust layer, smoke and soot particles from industrial emissions, and dew, which accumulate at different levels on the surface of the solar cell, cause negative effects on its performance by reducing the light receiving capacity of the panel [35].

In order to better understand the effects of pollutants deposited on solar cells and to minimise these effects, the classification of pollutants is of great importance. This classification facilitates the identification of pollution sources and seasonal changes. Pollutants can be generally divided into three main categories. The first category is pollutants of atmospheric origin and includes airborne particulate matter such as dust, smoke and soot. The second category consists of pollutants due to environmental factors. This group includes pollutants of natural origin such as hoarfrost, snow, pollen and organic materials. The third category consists of pollutants of local origin and includes substances such as particles emitted from industrial areas or soil transported from agricultural areas. Such categorisation allows the development of effective cleaning protocols for solar cells in a given geographical area.

The effects of air and surface pollution on the power supply systems of solar-powered UAVs should also be carefully analysed. The intensity and impact of pollutants are directly related to the mission duration of the UAV. While instantaneous pollution is usually negligible during short duration missions, pollutant accumulation becomes a significant problem during long duration missions and necessitates regular cleaning. Therefore, the effects of pollution should be evaluated by considering the time and mission duration parameters.

While some pollutants have instantaneous effects and cause short-term performance losses, others may cause permanent performance decreases in the long term. For example, while the accumulation of hoarfrost and snow in winter months temporarily reduces the radiation absorption capacity of solar cells, dust accumulation in summer months can cause longer and permanent performance losses. These effects are related to both atmospheric pollution and environmental factors and vary depending on seasonal variations [11].

2.5 Flight path and solar irradiation angle

The flight duration of solar-powered UAVs is directly related to solar irradiance angle and flight path optimisation. To achieve maximum energy generation, the irradiance angle must be maintained at an optimal level. The angle of incoming sunlight is determined by the aircraft's position, tilt angle and orientation. An optimal flight path should be designed considering these factors to ensure maximum solar irradiance exposure throughout the day [12].

https://doi.org/10.1017/aer.2026.10147 Published online by Cambridge University Press

Table 1. *Technical specifications of UAV with solar cells and UAV without solar cells models*

Parameter	UAV	SUAV
Wing span	4.00 m	4.00 m
Wing cord	0.312 m	0.312 m
Length	2.13 m	2.13 m
Height	0.43 m	0.43 m
Total mass	6.5 kg	7 kg
Battery mass	2.73 kg	2.73 kg
Cruise speed	31.48 km/h	31.90 km/h
Battery capacity	32000 mAh	32000 mAh
Solar cell area	–	1 m^2

In this study, gravitational potential energy utilisation is incorporated into flight path optimisation to extend the flight duration of solar-powered UAVs. Particularly during night flights, the excess energy harvested during the daytime allows the UAV to ascend to higher altitudes, accumulating potential energy. This stored energy is then gradually released during the night, enabling the UAV to glide downward efficiently, thereby optimising energy consumption and extending operational endurance [13].

Additionally, meteorological variables must be considered during flight path planning. For instance, UAVs operating at lower altitudes are more susceptible to atmospheric variations, while determining the optimal flight angle and altitude enhances long-term endurance. Real-time optimisation algorithms can continuously adjust the UAV's flight path by accounting for variables such as wind conditions, air density and cloud cover. The optimisation of flight trajectory and solar irradiance angle is regarded as a critical parameter for maximising energy harvested from solar cells and extending the UAV's flight duration [41].

3.0 Materials and methods – simulation model

In this study, a simulation model was developed to evaluate the effects of solar cell integration on energy consumption, flight duration and battery management in fixed-wing UAVs. The simulation models flight dynamics by considering the aerodynamic performance, energy management system and environmental factors of the UAV.

3.1 UAV characteristics

To compare two different flight scenarios, two UAV models with identical physical characteristics and aerodynamic parameters were utilised. The key distinction between these models is that one is equipped with solar cells integrated into the wing surface, while the other operates solely on battery power. Additionally, the integration of solar cells on the wing surface results in a 500 g increase in weight. The fundamental technical specifications of the UAV models used in this study are presented in Table 1.

Table 1 presents the main technical specifications of the two UAV configurations analysed in this study: the conventional UAV (without solar cells) and the solar-powered UAV (SUAV). Both platforms share the same geometric characteristics, featuring a wingspan of 4.0 m, a mean aerodynamic chord of 0.312 m and an overall fuselage length of 2.13 m with a height of 0.43 m.

The total mass of the conventional UAV is 6.5 kg, whereas the solar-powered variant weighs 7.0 kg due to the addition of solar modules and related power electronics. Both configurations utilise the same battery system, consisting of 60 Panasonic NCR18650B Li-ion cells connected in a 6S10P configuration, providing a total capacity of 32 Ah (32,000 mAh) and a battery mass of 2.73 kg. The cruise speed for the UAV and SUAV is approximately 31.48 km/h and 31.90 km/h, respectively. The SUAV version

https://doi.org/10.1017/aer.2026.10147 Published online by Cambridge University Press

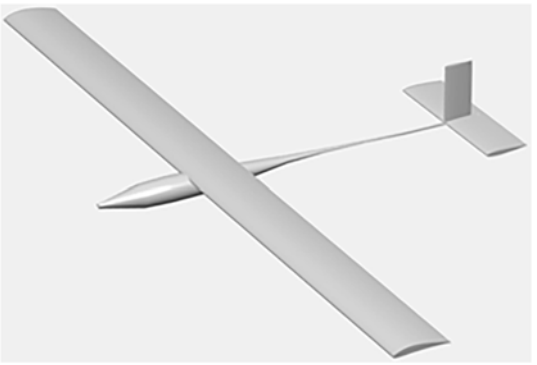


Figure 4. *General configuration of the designed UAV with NACA 6412 aerofoil and conventional tail layout.*

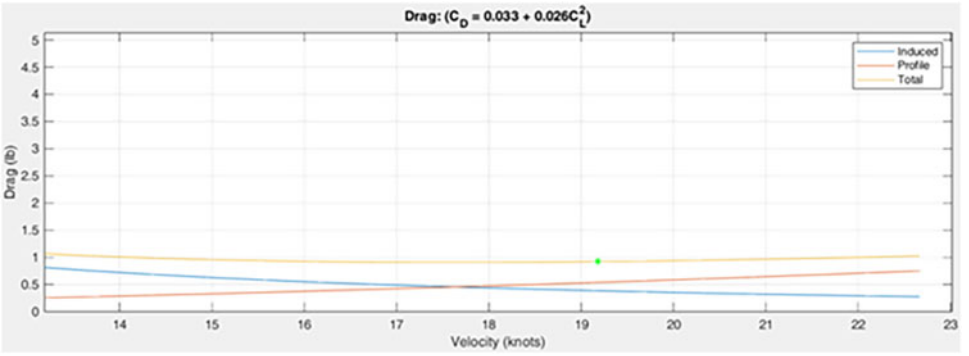


Figure 5. *Variation of induced, profile and total drag with velocity for the designed UAV.*

includes PV cells covering an active surface area of approximately 1 m^2, installed on the upper surface of the wings, which contributes to in-flight power generation and enhanced endurance. These specifications ensure that both aircraft are aerodynamically identical, allowing direct comparison of performance differences solely due to the inclusion of solar energy harvesting.

Figure 4 illustrates the geometric configuration of the designed fixed-wing UAV, which was developed for low-altitude, long-endurance solar-powered missions. The UAV features a high-aspect-ratio straight wing with a 4.0 m wingspan and a mean aerodynamic chord of approximately 0.31 m. The selected NACA 6412 aerofoil provides balanced lift-to-drag performance in the low Reynolds number range ($Re \approx 2 \times 10^5$), supporting efficient low-speed flight and stable loitering. The fuselage length is 2.13 m, accommodating the flight control electronics, battery pack and power electronics. A conventional tail configuration was selected to ensure control effectiveness, simplicity of construction and ease of maintenance during field operations. The SUAV version includes solar cells mounted on the upper surface of the wing, resulting in a total active PV area of approximately 1 m^2, as detailed in Table 1.

The aerodynamic characteristics of the UAV were analysed using the NACA 6412 aerofoil, which provides a favourable lift-to-drag ratio in the low Reynolds number regime ($Re \approx 2 \times 10^5$). The total drag was modeled as the sum of induced and profile drag, and the resulting drag polar was expressed as $C_D = 0.033 + 0.026C_L^2$, where the constant term represents profile drag while the quadratic term accounts for the induced drag contribution.

Figure 5 presents the variation of drag components with velocity. The minimum total drag occurs near a flight speed of 17–18 kn (8.7–9.3 m/s), identified as the cruise condition. At this point, the lift and drag coefficients are $C_L \approx 0.68$ and $C_D \approx 0.045$, respectively, yielding an efficient lift-to-drag ratio suitable for long-endurance low-speed flight.

https://doi.org/10.1017/aer.2026.10147 Published online by Cambridge University Press

3.2 Power consumption analysis

In the simulation model of the UAV, power consumption is evaluated under three main components: propulsion system, avionics systems and auxiliary electronic systems. The total energy consumption of the UAV varies depending on the flight scenario, operational conditions and environmental factors. In this context, various assumptions and systematic modeling approaches were used in power consumption calculations during the simulation process.

The propulsion system is the highest power-consuming component in the model and includes the energy consumed by the electric motors. This energy consumption reaches its highest level during the takeoff and climb phases, approaches a relatively constant value during cruise flight, and decreases to a minimum level during the glide phases. In the model, it is assumed that the power consumption of the electric motors during gliding can be neglected.

Avionic systems include the fixed energy consumption required for the control, navigation and communication systems of the UAV. In the simulation, the power consumption of the electric motors is considered as a variable, while the power consumption of the avionics systems is modeled as a fixed value. Although the total energy consumption of the avionics systems is a low percentage compared to the propulsion system, it is included in the total power consumption calculations of the model.

In the simulation model, four main subsystems are defined to calculate the power consumption of the UAV. These are Flight Control Unit (FCU), environmental model, airframe dynamics and power management system. The FCU manages the mission scenario of the UAV and determines the required flight parameters. The environmental model calculates environmental variables depending on the flight altitude and atmospheric conditions. The airframe dynamics determines the required torque and power demand using data from the flight control module and the environmental model. The power management system manages the total energy consumption of the UAV and calculates the energy balance provided by the battery and solar cell.

The working principle of the implemented model can be explained as follows: the FCU determines the altitude changes appropriate to the flight scenario by taking into account the environmental variables. The environmental model calculates the lift-and-drag forces, depending on the atmospheric conditions. The body dynamics determines the torque and power demand required by the engine using these inputs. Finally, the power management system optimises the energy balance provided by the battery and solar cell to meet the power needs of the propulsion system and avionics components.

The modeled energy management system of the solar-powered UAV is illustrated in Fig. 6, detailing its components and functionality. The system diagram presented in Fig. 6 depicts an integrated structure that encompasses solar energy conversion, power transformation, energy storage and consumption processes. The model consists of four main components: the propulsion system, energy conversion systems, battery management and avionics components.

The primary energy source of the UAV is provided by PV solar cells integrated into the wing surface. These cells convert solar irradiation into electrical energy, thereby meeting the power requirements of the system. However, the efficiency of solar cells is influenced by various environmental factors, including irradiation levels, temperature, cloud cover and air pollution.

The primary energy source of the UAV is provided by PV solar cells integrated into the wing surface. These solar cells convert solar irradiation into electrical energy, thereby meeting the power requirements of the system. However, the efficiency of solar cells is influenced by various environmental factors, including irradiation levels, temperature, cloud cover and air pollution.

The energy generated by the solar cells is regulated to meet the UAV's power requirements through DC/DC converters. These converters not only facilitate the charging of the battery system but also ensure proper energy distribution by supplying appropriate power levels to the propulsion and avionics systems.

The energy harvested from the solar cells is stored in the energy storage system, ensuring a continuous power supply throughout the flight. The optimal management of the batteries plays a critical role in extending the flight duration.

In this context, the energy storage management system continuously monitors the state of charge (SoC) of the battery and regulates the energy flow to ensure efficient power distribution. The output data

https://doi.org/10.1017/aer.2026.10147 Published online by Cambridge University Press

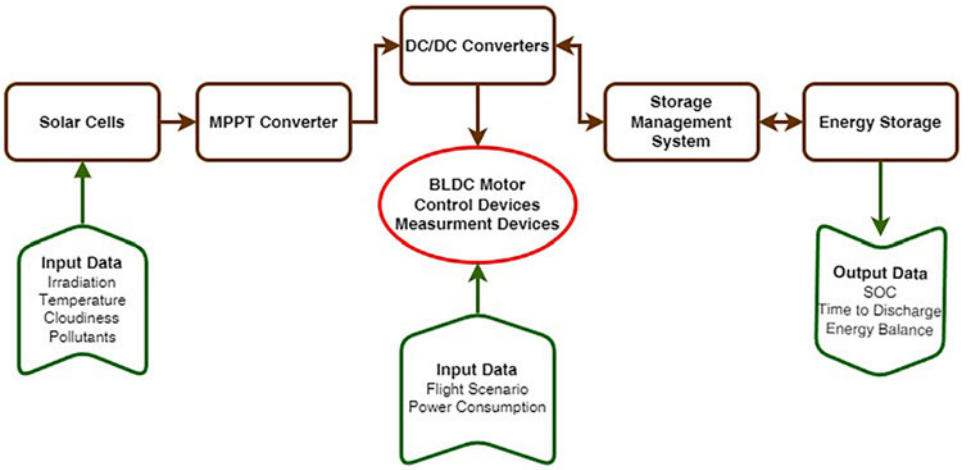


Figure 6. *General energy management diagram.*

of the model includes several key parameters. The SoC represents the current charge level of the battery, providing insights into its available capacity. The time to discharge indicates the estimated operational duration of the battery based on the current power consumption. Additionally, the energy balance reflects the equilibrium between the generated and consumed energy, ensuring optimal energy utilisation within the system. These data are utilised to optimise the UAV's energy consumption and ensure operational continuity.

The model is designed to maximise the efficient utilisation of energy harvested from solar cells, ensure effective battery management and optimise the power requirements of the propulsion system. The FCU determines the energy demand by considering environmental variables, while the energy management system balances the energy supplied from the battery and solar cells accordingly. Aimed at optimising the power management processes of solar-powered UAVs, the model focuses on analysing the impact of battery capacity and solar energy generation on flight duration, without directly targeting range or aerodynamic performance.

The model is designed to maximise the efficient utilisation of energy harvested from solar cells, ensure effective battery management and optimise the power requirements of the propulsion system. The FCU determines the energy demand by considering environmental variables, while the energy management system balances the energy supplied from the battery and solar cells accordingly. Aimed at optimising the power management processes of solar-powered UAVs, the model focuses on analysing the impact of battery capacity and solar energy generation on flight duration, without directly targeting range or aerodynamic performance.

3.3 Power supply elements

3.3.1 Solar cells

In this study, SunPower C60 solar cells were utilised to meet the UAV's energy requirements. These cells are distinguished by their high efficiency, lightweight structure and durability. According to the manufacturer's specifications, the maximum efficiency of these cells is 22.5%, with each unit generating approximately 3.46 W of power. Each SunPower C60 monocrystalline silicon cell has physical dimensions of approximately 125 mm × 125 mm and an average mass of 3 g per cell, providing a compact and lightweight design suitable for UAV applications [42].

A total of 64 SunPower C60 solar cells were installed on the UAV's wing surface. The configuration of the solar cells connections was determined by considering the nominal voltage of the battery and the voltage range of the maximum power point tracking (MPPT) converter. Parallel and series connection

https://doi.org/10.1017/aer.2026.10147 Published online by Cambridge University Press

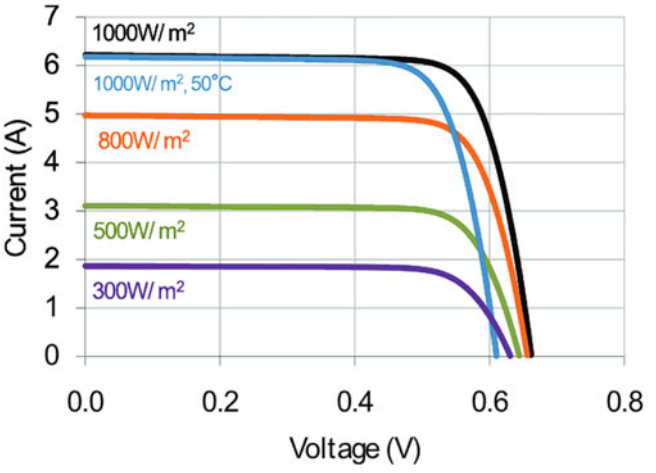


Figure 7. *Irradiation-dependent I-V characteristics of the SunPower C60 solar cell [43].*

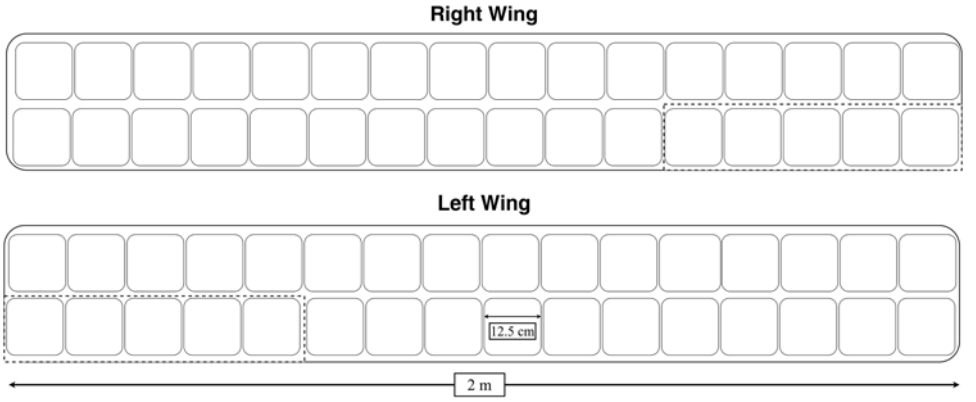


Figure 8. *Solar cell layout on the UAV wings showing the 32S2P configuration. Dashed lines represent aileron boundaries.*

options were evaluated to select the most optimal configuration. Figure 7 presents the voltage-current (V-I) characteristics of the SunPower C60 solar cell, illustrating its performance under varying irradiation levels and temperature conditions.

During the integration of the solar cells onto the UAV's wing surface, a 100 μm thick polyvinyl chloride (PVC) coating was applied to enhance mechanical durability and provide protection against environmental factors. Although this coating causes a slight decrease in the efficiency of the solar cells, it significantly improves their resistance to impacts, weather conditions and wear over long-term use.

In the series connection structure of the solar cells, it was considered that the current value of the entire connection chain could decrease if a single cell were damaged. To enhance the system's durability, parallel connection options were evaluated, providing redundancy in energy production. As a result, even in the event of a cell failure, the impact on the total energy production of the system was minimised.

The solar PV modules are installed exclusively on the upper surfaces of the left and right wings, as illustrated in Fig. 8. The panels are arranged symmetrically along a total wingspan of 4 m, ensuring uniform exposure to solar irradiance during level flight. The dashed lines in the figure indicate the boundaries of the ailerons. This configuration allows efficient utilisation of the available wing surface area for maximum solar energy harvesting.

In the final configuration, each wing incorporates 32 solar cells connected in series, providing a nominal voltage suitable for the UAV's DC/DC converter input. The left and right wings are connected in

https://doi.org/10.1017/aer.2026.10147 Published online by Cambridge University Press

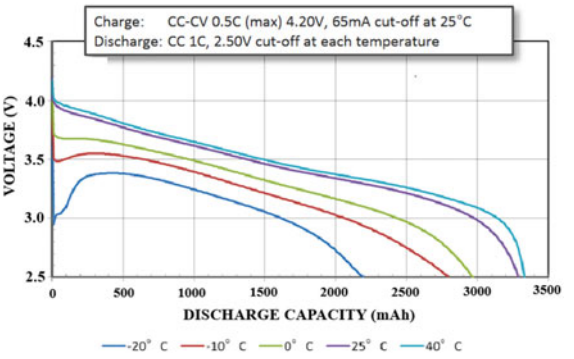


Figure 9. *Discharge performance of the NCR18650B lithium-ion battery based on temperature variation* [45].

parallel, resulting in an overall 32S2P configuration. This design ensures symmetrical power generation from both wings and provides a balanced voltage and current output for the power management and storage subsystems.

3.3.2 Battery cells

In this study, a battery pack was created for the UAV using Panasonic NCR18650B Li-ion battery cells, which are distinguished by their high energy density, lightweight design and long cycle life. These cells provide a nominal voltage of 3.6V, a capacity of 3200mAh, and a maximum continuous discharge current of 4.87A. Furthermore, these cells, which maintain up to 80% of their capacity for up to 500 cycles, can operate safely over a wide temperature range (−20°C) to (60°C).

To meet the energy requirements of the UAV, a total of 60 battery cells were arranged in a 6S10P configuration. This structure provides a system voltage of 21.6V through series connections, while the parallel connections enable the total capacity to reach 32Ah. This configuration is ideal for high power output, stable voltage balance and long flight durations [10].

Studies in the literature have reported that the SoC of Li-ion batteries is temperature-sensitive, with approximately a 23% decrease when the temperature drops from (25°C) to (−15°C) [39]. Therefore, temperature-dependent battery performance and energy efficiency calculations were considered and integrated into the numerical analysis and simulation environment.

According to data obtained from the General Directorate of Meteorology in Turkey, the average night temperatures in Kayseri province during the summer months range between 12°C and 14°C. Since the flights are planned to be conducted at an altitude of 1000 meters in the simulation, it is expected that the ambient temperature during level flight will be approximately 6°C lower. Accordingly, it is anticipated that the average ambient temperature during flights after sunset will be around 6°C to 8°C [44].

Figure 9 presents the temperature-dependent discharge curves of the Panasonic NCR18650B Li-ion battery, illustrating the variation in capacity and voltage under different thermal conditions. Especially at temperatures below 0°C, there is a considerable decline in the battery's energy storage and transmission capacity. To achieve optimal performance, it is recommended that the battery be used within temperature range of 25°C to 40°C.

In this study, the expression provided in Equation (18) was used to calculate how the battery capacity is affected by temperature variations. In this expression, C_{eff} represents the available battery capacity at the current temperature, C is the nominal capacity of the battery, T is the ambient temperature and the coefficient 0.006 represents the capacity loss that occurs as the temperature increases [46]. While this coefficient is not a precise value, it is presented as a generalised approach based on studies in literature.

$$C_{eff} = C\,x\ (1 - 0.006 \times (T - 25)) \tag{19}$$

https://doi.org/10.1017/aer.2026.10147 Published online by Cambridge University Press

The total energy calculation E_t is determined using the following formulas. Here, V_t resents the total voltage of the battery pack, S is the number of cells connected in series, V_n is the nominal voltage of a single cell, C_t is the capacity of a single cell and P denotes the number of cells connected in parallel.

$$V_t = S\,x\,V_n$$

$$C_t = P\,x\,C_{eff} \tag{20}$$

$$E_t = V_t\,x\,C_t$$

This 6S10P battery pack is designed to meet the energy requirements of the UAV during flight. The total energy capacity of the battery provides sufficient power for long duration flights. Furthermore, the high capacity and series connection arrangement offer a stable power source for the motors and other flight systems.

The battery pack, working in conjunction with the solar cells during flight, has created a hybrid energy system. The energy generated by the solar cells allows for the recharging of the battery, optimising energy consumption. Additionally, by using an energy management system, the voltage and current levels of the battery were kept under control, thereby enhancing system safety.

3.4 Simulation model

In this study, the flight simulation model developed for the solar-powered UAV was created to analyse the interaction between aircraft dynamics, energy management and environmental factors. The flowchart presented in Fig. 10 outlines the key components and decision mechanisms of the simulation process.

The simulation process begins with the initialisation of the aircraft parameters (UAV, environmental conditions and mission definitions), followed by two key external factors: the generation of weather data and the calculation of solar energy. The energy harvested from the solar cells is calculated in coordination with the battery management system (BMS), determining the available power for use during the flight.

Subsequently, aerodynamic calculations such as lift, drag and power requirements are performed, and the aircraft's position, speed and energy status are continuously updated. Throughout the flight process, factors that may lead to the termination of the flight, such as battery status, reaching target points and energy consumption, are monitored. These target points are planned such that the flight will last more than 24 hours.

In the simulation model, the transition to landing and the termination of the flight occur either when the battery level drops below 10% or when the aircraft reaches its target point. If the battery level is sufficient and the flight process continues, calculations are made to maintain cruising altitude and speed. The flight dynamics are updated, and the process continues cyclically.

3.5 Flight path scenarios

In this study, flight path scenarios were developed for two different UAVs with the same physical characteristics and initial parameters. One of these aircraft, capable of generating energy through solar cells during flight, is referred to as the SUAV. The other UAV operates solely by utilising the energy stored in its battery at the beginning, without any additional energy generation mechanism. The developed flight scenarios were modeled considering the flight altitude, energy management and battery SoC for both the SUAV and the UAV without solar cells.

The flight path scenario developed for the solar-powered UAV is based on a dynamic model that varies depending on the battery status and flight altitude. The flowchart presented in Fig. 11 illustrates how the UAV operates in terms of altitude management, SoC and flight strategies. According to the diagram, the flight scenario begins with the definition of the UAV's starting position, followed by the climb phase. Once the UAV reaches an altitude of 1000 meters, the level flight mode is activated. While continuing flight at this altitude, the SoC is continuously monitored. When the SoC reaches 99% or

https://doi.org/10.1017/aer.2026.10147 Published online by Cambridge University Press

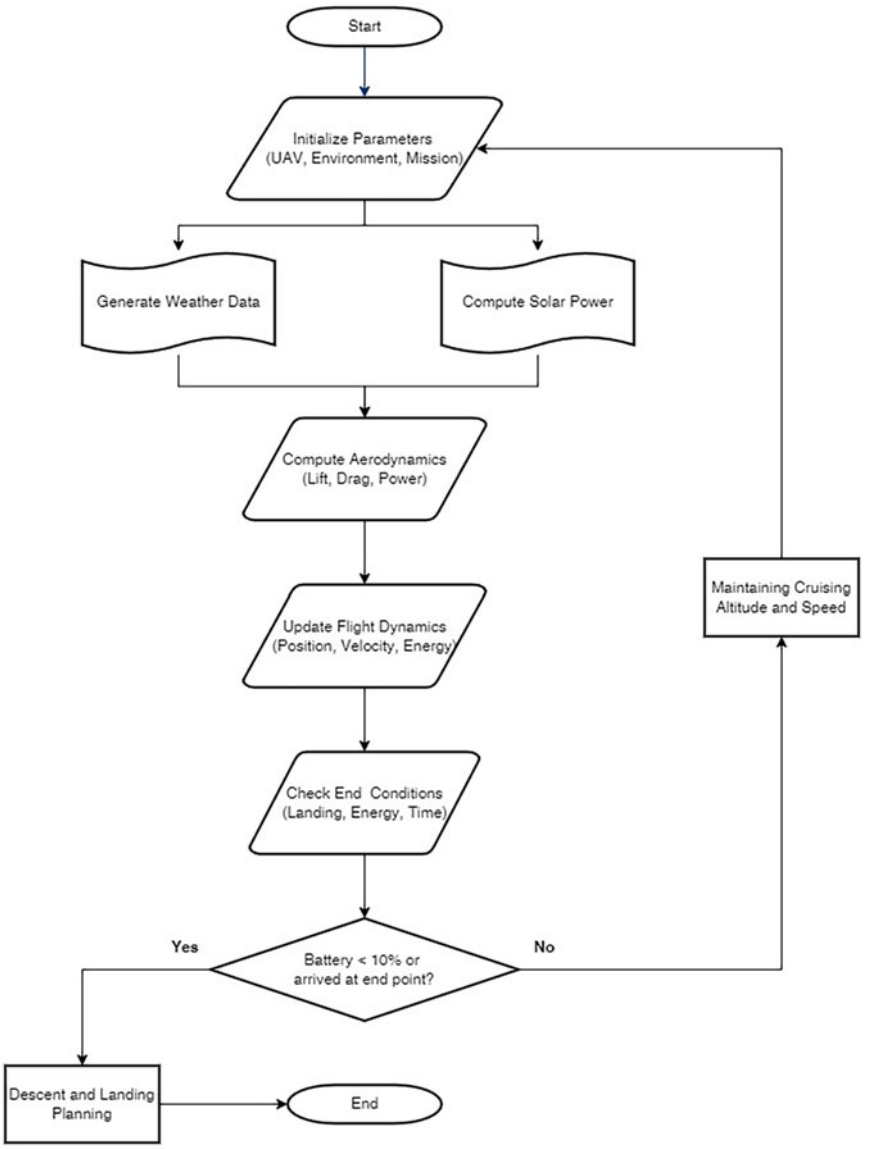


Figure 10. *Basic components and decision mechanisms of the simulation process.*

higher, the UAV initiates a second climb to reach a higher altitude, targeting 2000 meters. If the battery level falls below 98%, in order to maintain energy efficiency, the UAV descends back to 1000 meters and continues flying at this altitude.

On the other hand, when the SoC drops to 10% or lower, the UAV enters the descent phase. If the battery level rises above 10%, the flight continues at the current altitude. However, if the battery level falls below 10%, the landing phase is initiated, and the flight is terminated.

This flight scenario is based on dynamically changing two different altitude levels in terms of energy management. The solar-powered UAV can fly at higher altitudes when sufficient energy is produced, and when the battery level decreases, it transitions to a lower altitude to optimise energy consumption. This ensures that flight duration is maximised and energy management is maintained at an optimal level. On the other hand, the UAV without solar cells operates solely based on the initial battery capacity and does

https://doi.org/10.1017/aer.2026.10147 Published online by Cambridge University Press

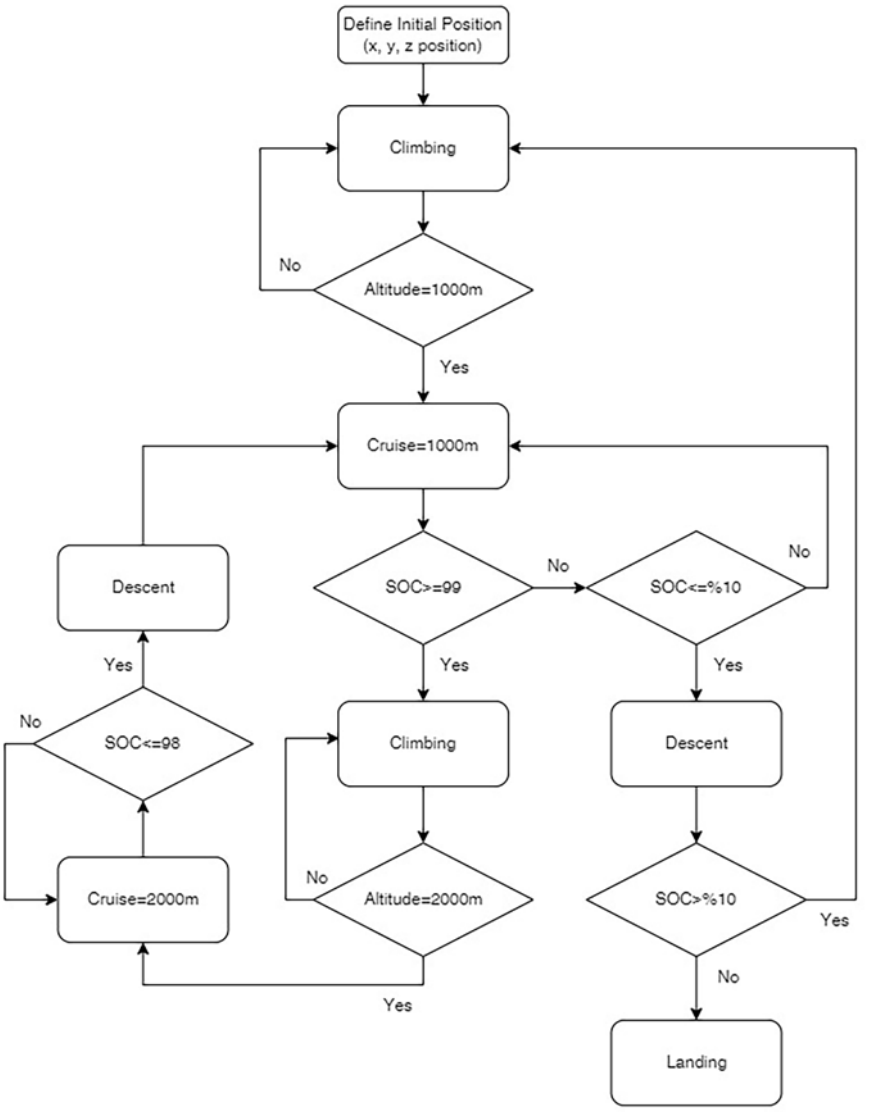


Figure 11. *Altitude control algorithm for the solar-powered UAV. The flowchart outlines the decision logic governing climb, cruise and descent phases based on altitude targets and battery state of charge (SoC) thresholds, ensuring energy-aware and continuous flight operation.*

not generate energy during flight. After climbing to 1000 meters, this UAV transitions to level flight and continues the flight duration depending on the battery level. However, since there is no energy generation mechanism, when the SoC falls below 10%, the landing procedure is initiated.

This modeling demonstrates comparative analysis of the effects of solar energy utilisation on the operational durations and flight altitudes of UAVs. Specifically, the SUAV is able to dynamically manage its flight altitude and duration using the energy provided by the solar cells, thereby increasing energy usage efficiency. In contrast, the UAV without solar cells operates based on battery capacity, resulting in a more limited operational profile in terms of flight duration and altitude management.

https://doi.org/10.1017/aer.2026.10147 Published online by Cambridge University Press

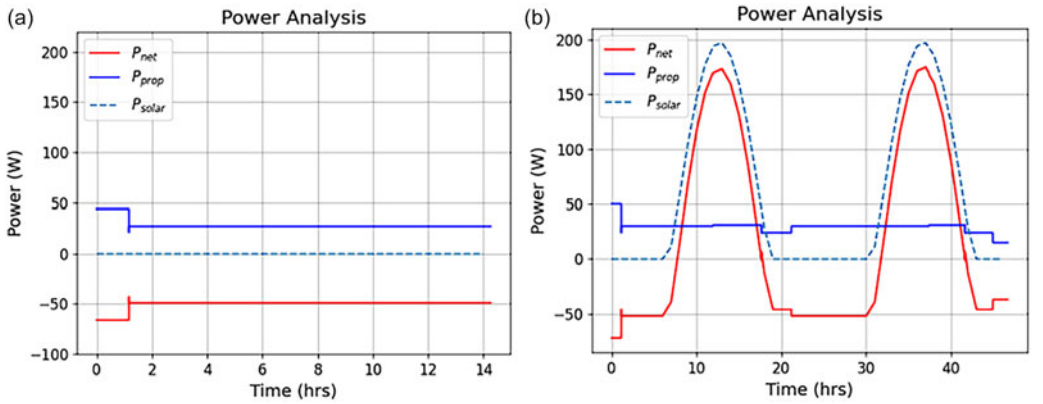


Figure 12. *(a) Power analysis of UAV without solar cells. (b) Power analysis of UAV with solar cells.*

4.0 Results and discussion

4.1 Power consumption analysis

In this study, a power consumption analysis has been conducted for two UAVs with the same physical characteristics and flight scenarios. The only difference is that one UAV is equipped with solar cells, while the other model is without solar cells and is 500 g lighter. Figure 12(a) and (b) presents the power consumption analysis of UAVs with and without solar cells, respectively.

Examining the graphs in Fig. 9, it is evident that the power consumption dynamics of the solar-powered UAV vary depending on solar irradiation. The solar energy produced during the day, P_{Solar}, partially meets the energy requirements of the motor and other systems, thereby reducing the load on the battery. During the night or under low irradiation levels, when the solar cells are unable to generate energy, the UAV becomes fully dependent on battery power.

In contrast, the power consumption graph of the UAV without solar cells shows a constant and continuous energy consumption, as this model relies solely on battery power. The changes in power consumption are observed to be dependent on the flight dynamics; however, since there is no external energy source, the P_{Solar} component is zero.

The UAV without solar cells is 500 g lighter, which results in a reduction in the total power demand of the propulsion system. However, this difference does not provide a significant advantage for long duration flights, as the energy consumed from the battery continues to decrease at a steady rate.

On the other hand, despite the increased weight disadvantage, the solar-powered UAV demonstrates a longer flight duration due to the support provided by solar energy. The additional energy derived from the solar cells compensates for the power requirement caused by the weight difference, making the overall energy balance more sustainable.

The solar-powered UAV has an energy management system that reduces battery consumption and increases flight duration. Although the UAV without solar cells is lighter, its dependence on the battery results in a more limited flight time. The energy produced by the solar cells contributes to maintaining the battery capacity and allows for recharging during daylight hours. While the weight difference may impact energy consumption in the short term, the operational advantages of the solar-powered system, which ensures sustainable energy production, become more apparent in the long term.

4.2 Battery cell efficiency

In order to simplify the simulation model, the effects of temperature have been integrated into the model; however, the degradation effects of the battery have not been considered. This is because the capacity loss during the operational period of the system remains below a certain threshold, and the decrease in battery capacity after several hundred charge and discharge cycles is negligible [11]. With this approach,

https://doi.org/10.1017/aer.2026.10147 Published online by Cambridge University Press

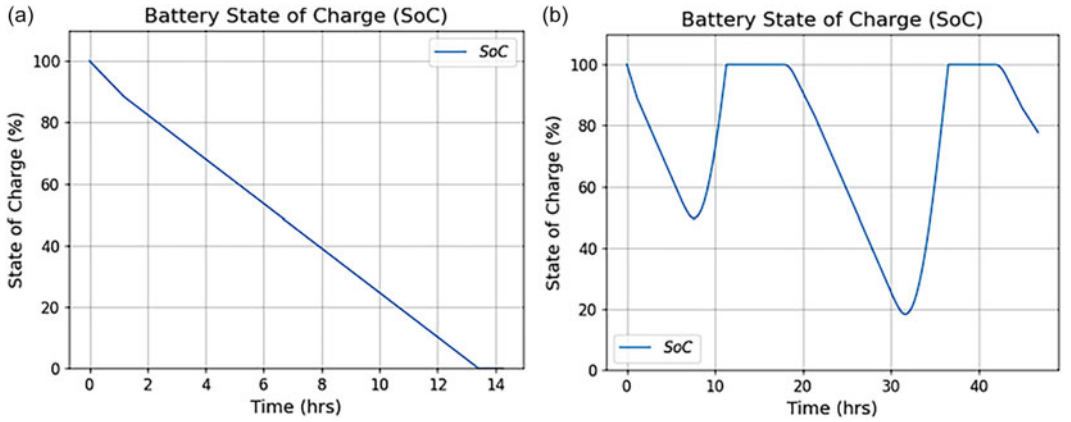


Figure 13. *(a) Time-dependent variation in the SoC for the UAV without solar cells. (b) Time-dependent variation in the SoC for the UAV with solar cells.*

the ability of the model to represent real systems in practice has been enhanced, and the changes in battery performance under different operational conditions have been analysed with greater accuracy.

In this study, the SoC of two UAV models with the same physical properties – one with solar cells and the other powered solely by the battery – has been analysed. In Fig. 13(a) and (b), the time-dependent variation of the SoC for the solar-powered UAV and the UAV without solar cells is shown, respectively. The SoC of the solar-powered UAV follows a variable trend, depending on solar irradiation. The periodic fluctuations observed in the SoC curve indicate that during daylight hours, the solar cells charge the battery, while at night, energy is consumed from the battery. During periods of high solar irradiation (daytime), the battery is charged, and the SoC reaches 100%. At night or during low irradiation conditions, since energy consumption is solely from the battery, the SoC level decreases. Full charge and discharge cycles show that the battery can be recharged, and the energy management system remains sustainable. The battery level may drop to around 20%, but it is recharged by the solar cells, bringing the SoC back to 100%. This demonstrates that the solar-powered UAV significantly increases its operational duration and optimises battery consumption. Particularly in areas with sufficient solar irradiation, even when the battery level is low, energy production continues, thus extending the flight time.

The battery SoC of the UAV without solar cells exhibits a linear decrease over time. Due to the absence of energy generation, the battery is directly consumed without any recharging process. At the beginning of the flight, the SoC level is at 100%, but it continuously declines as time progresses. After approximately 14 hours, the battery is fully depleted, and the SoC level reaches 0%, indicating the end of the UAV's operational duration. Since there is no energy input from solar cells, the battery cannot be recharged once it is discharged, rendering the UAV inoperable.

4.3 Comparison of flight path and flight endurance

In this study, the flight paths and endurance durations of two different UAV models, one equipped with solar cells and the other without, were compared. Both UAV models share the same initial conditions, propulsion system and aerodynamic characteristics, with the primary distinction being that the solar equipped model can harness solar energy during flight to recharge its battery.

Figure 14(a) and (b) illustrates the variations in flight altitude over time for the UAV equipped with solar cells and the UAV without solar cells.

The UAV without solar cells initially ascends to an altitude of 1000 meters and maintains level flight until the battery is fully depleted. After approximately 14 hours of operation, when the battery level

https://doi.org/10.1017/aer.2026.10147 Published online by Cambridge University Press

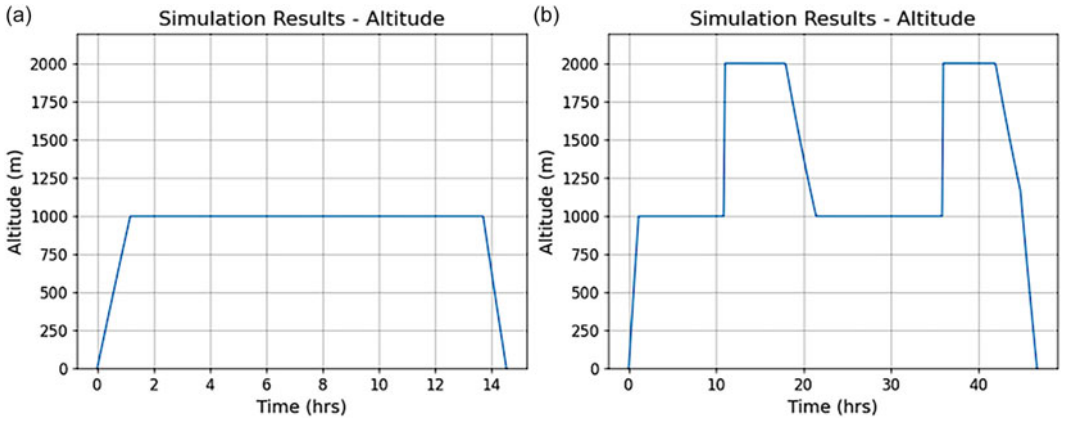


Figure 14. *(a) Time-dependent variation of flight altitude for the UAV without solar cells. (b) Time-dependent variation of flight altitude for the UAV with solar cells.*

reaches a critical threshold, the UAV initiates its descent. Since no additional energy generation is available, the flight duration is strictly limited by battery capacity. When the battery level drops below 10%, a safe landing procedure is executed.

In contrast, the flight path analysis of the solar-powered UAV reveals a more dynamic flight profile in terms of energy management. As long as the battery level remains sufficient, the UAV initially ascends to 1000 meters and transitions into level flight. During periods of high solar irradiance, when the battery is fully charged, the UAV climbs to 2000 meters to utilise the excess generated energy. When the battery level drops below a certain threshold, the UAV descends back to 1000 meters to optimise energy consumption. This process repeats throughout the day, forming a dynamic energy management strategy that extends the flight duration.

The solar-powered UAV successfully completed a 24-hour flight cycle, demonstrating its capability for continuous flight through effective solar irradiance utilisation and battery management. Although the simulation continued for 45 hours, the UAV's descent occurred not due to energy depletion but as a result of reaching its designated destination in the operational scenario. This finding suggests that, under appropriate flight strategies and sufficient solar irradiance conditions, a solar-powered UAV could potentially achieve indefinite flight endurance.

According to the simulation results, the solar UAV optimised battery consumption, completed a full 24-hour cycle, and theoretically demonstrated the capability for indefinite flight under suitable temperature and irradiance conditions In contrast, the UAV without solar cells, being entirely dependent on its initial battery capacity, could sustain operation for only 14 hours before being forced to land due to complete battery depletion. By dynamically adjusting its altitude, the solar UAV optimised energy management, utilised excess energy efficiently and ensured operational continuity. During daylight hours, when solar irradiance was available, battery charging enabled extended flight durations.

5.0 Conclusion

This study investigates the effects of solar cells on the flight duration, power consumption and battery management of a fixed wing UAV. Two UAV models with identical aerodynamic characteristics were compared: one powered solely by battery energy and the other equipped with solar cells for additional energy generation. The simulation results demonstrated that solar cells significantly contribute to UAV energy management and play a crucial role in extending flight duration. This model was developed to analyse how solar-powered UAVs can be optimised in terms of flight dynamics, energy management and operational sustainability. Particularly in terms of battery management and aerodynamic calculations,

https://doi.org/10.1017/aer.2026.10147 Published online by Cambridge University Press

the model provides a realistic assessment, helping to balance energy production and consumption and facilitating the modeling of long-term and sustainable flight scenarios.

According to power consumption analyses, the battery powered UAV exhausted its energy after approximately 14 hours of flight, constrained by battery capacity. In contrast, the solar-powered UAV was able to utilise solar energy during daylight hours to recharge its battery, reaching full capacity and completing a 24-hour flight cycle. This result indicates that, under sufficient irradiance conditions, continuous flight is theoretically possible. However, the UAV's 24-hour continuous flight capability is not solely dependent on daylight duration or irradiance levels. Since battery capacity fluctuates with ambient temperature, lower temperatures can reduce flight duration. For this reason, the simulations were conducted during summer conditions.

SoC analyses have demonstrated that solar cells help maintain the SoC level, enabling extended flight durations. While the battery level of the UAV without solar cells decreases linearly until depletion at the end of the flight, the battery in the solar-powered model is recharged during daylight hours, and energy consumption is optimised during nighttime, thereby extending the operational duration.

In terms of flight altitude, it has been observed that the solar-powered UAV ascends to 2000 meters when excess energy is available, increasing its potential energy, and descends to 1000 meters when the battery level decreases to optimise energy consumption. This dynamic flight management strategy enhances energy efficiency and extends operational duration. In contrast, the UAV without solar cells remains at a constant altitude of 1000 meters, solely dependent on battery capacity, and continues its flight until the battery is depleted. The integration of solar cells emerges as a crucial factor in extending the flight duration and operational efficiency of fixed wing UAVs. By utilising solar energy, battery consumption is optimised, flight duration is extended and energy management becomes more sustainable. This study highlights the potential of renewable energy supported aerial vehicles for long duration operations, particularly in reconnaissance, surveillance and logistics applications. Future research may focus on evaluating the performance of solar cells under different geographical and atmospheric conditions and optimising energy management strategies.

This study highlights the potential of renewable energy supported UAVs for long duration operations, particularly in reconnaissance, surveillance and logistics applications. Future research may focus on evaluating solar cell performance under different geographic and atmospheric conditions and optimising energy management strategies.

The present study established a numerical framework to evaluate the impact of solar energy integration on the performance of a fixed-wing UAV under representative summer conditions for the Central Anatolia region. The developed simulation model incorporates key environmental factors such as solar irradiance, temperature and cloud cover and provides a reliable analytical basis for understanding the energy balance of solar-powered UAVs. However, this work is limited to numerical validation, and real flight testing has not yet been performed. As part of future research, limited experimental flights will be conducted to validate the simulation outcomes. In addition, to mitigate the high cost of solar panels and reduce the risk of airframe damage, a ground-based test bench will be developed to emulate real flight loads and irradiance conditions, enabling controlled performance evaluations. Furthermore, Monte Carlo and sensitivity analyses will be carried out to assess the influence of stochastic weather variations and model uncertainties, while the framework will be extended to cover different geographical regions and seasonal conditions. These efforts aim to achieve a comprehensive and experimentally supported understanding of the long-endurance potential of solar-powered UAVs.

Future studies could explore solar cell performance under various environmental and operational scenarios, optimise battery management algorithms and integrate next generation energy solutions into UAV systems. Additionally, new systems could be developed to ensure battery operation is unaffected by external temperatures and to enable 24-hour continuous flight even in winter conditions with shorter daylight durations. Advancements in this direction will further enhance the viability of solar energy for long duration reconnaissance, surveillance and autonomous aerial vehicles, laying the foundation for sustainable aviation in the future.

https://doi.org/10.1017/aer.2026.10147 Published online by Cambridge University Press

Acknowledgements. The authors would like to thank the Erciyes University Scientific Research Projects Unit for their financial support (Project No: FDK-2024-13545).

References

[1] Guizani, S. Low energy system proposal for UAV applications using flexible solar cells, 15th International Wireless Communications & Mobile Computing Conference (IWCMC)*, IEEE*, 2019, pp 455–458.
[2] Hasan, F.H., Algburi, S. and Ezzat, S.B. Investigating the impact of internal and external factors on solar cell performance to enhance energy conversion efficiency, *NTU J. Renew. Energy*, 2025, **8**, pp 14–23.
[3] Kasi, S.V., Das, N., Alahakoon, S. and Hassan, N. Effective sizing and optimization of hybrid renewable energy sources for micro distributed generation system, *IET Renew. Power Gener*, 2025, **19**, p 13193.
[4] Wu, Z. Overview and energy power analysis of composite solar unmanned aerial vehicles, *Adv. Eng. Technol. Res.*, 2024, **9**, pp 281–281.
[5] Al Dhafari, L.S., Afzal, A., Al Abri, O.K. and Khan, A. Solar-powered UAVs: a systematic literature review, 2nd International Conference on Unmanned Vehicle Systems-Oman (UVS), 2024, pp 1–8.
[6] Hamza, A., Mohammed, A. and Isah, A. Towards solar-powered unmanned aerial vehicles for improved flight performance, *2nd International Conference of the IEEE Nigeria Computer Chapter (NigeriaComputConf),* 2019, pp 1–5.
[7] Li, S. Advanced algorithms for autonomous guidance of solar-powered UAVs, arXiv preprint arXiv:2404.02920, 2024.
[8] Tian, Z., Haas, Z.J. and Shinde, S. Routing in solar-powered UAV delivery system, *Drones*, 2022, **6**, p 282.
[9] Oettershagen, P., Melzer, A., Mantel, T., Rudin, K., Stastny, T. and Wawrzacz, B. Perpetual flight with a small solar-powered UAV: flight results, performance analysis and model validation, *IEEE Aerospace Conference, IEEE*, 2016, pp 1–8.
[10] Oettershagen, P., Melzer, A., Mantel, T., Rudin, K., Stastny, T., Wawrzacz, B., Hinzmann T., Leutenegger, S., Alexis, K. and Siegwart, R. Design of small hand-launched solar-powered UAVs: from concept study to a multi-day world endurance record flight, *J. Field Rob.*, 2017, **34**, (7), pp 1352–1377.
[11] Mateja, K., Skarka, W., Peciak, M., Niestrój, R. and Gude, M. Energy autonomy simulation model of solar powered UAV, *Energies*, 2023, **16**, p 479.
[12] Huang, Y., Chen, J., Wang, H. and Su, G. A method of 3D path planning for solar-powered UAV with fixed target and solar tracking, *Aerosp. Sci. Technol.*, 2019, **92**, pp 831–838.
[13] Lee, J.S. and Yu, K.H. Optimal path planning of solar-powered UAV using gravitational potential energy, *IEEE Trans. Aerosp. Electron. Syst.*, 2017, **53**, pp 1442–1451.
[14] Fernandes, P., Santos, R. and Rego, F. Experimental evaluation of UAV energy management using solar panels and battery systems, *Appl. Sci.*, 2025, **15**, p 10689.
[15] Zhang, C., Zhang, C., Li, L. and Guo, Q. Parameter analysis of power system for solar-powered unmanned aerial vehicle, *Appl. Energy*, 2021, **295**, p 117031.
[16] Gao, Y., Qiao, Z., Pei, X., Wu, G. and Bai, Y. Design of energy-management strategy for solar-powered UAV, *Sustainability*, 2023, **15**, p 14972.
[17] Kalogirou, S.A. *Solar Energy Engineering: Processes and Systems*, 2013, London, United Kingdom: Elsevier.
[18] Rydh, C.J. and Sandén, B.A. Energy analysis of batteries in photovoltaic systems. Part I: performance and energy requirements. *Energy Convers. Manag*, 2005, **46**, pp 1957–1979.
[19] Rydh, C.J. and Sandén, B.A. Energy analysis of batteries in photovoltaic systems. Part II: energy return factors and overall battery efficiencies, *Energy Convers. Manag*, 2005, **46**, pp 1980–2000.
[20] Aktas, A. and Kirçiçek, Y. Chapter 13-Examples of solar hybrid system layouts, design guidelines, energy performance, economic concern, and life cycle analyses, in Hayton, J. and Reading, L. (Eds.), *Solar Hybrid Systems*. Academic Press, 2021, Cambridge, MA, USA, pp 331–349.
[21] Duffie, J.A., Beckman, W.A. and Blair, N. *Solar Engineering of Thermal Processes, Photovoltaics and Wind*, 2020, Hoboken, NJ, USA: John Wiley & Sons.
[22] Page, J. The role of solar-radiation climatology in the design of photovoltaic systems, Practical Handbook of Photovoltaics, 2012, pp 573–643.
[23] Hottel, H.C.A. Simple model for estimating the transmittance of direct solar radiation through clear atmospheres. *Sol. Energy*, 1976, **18**, pp 129–134.
[24] Eissa, Y., Marpu, P.R., Gherboudj, I., Ghedira, H., Ouarda, T.B.M.J. and Chiesa, M. Artificial neural network based model for retrieval of the direct normal, diffuse horizontal and global horizontal irradiances using SEVIRI images, *Sol. Energy*, 2013, **89**, pp 1–16.
[25] Dumka, U.C., Kosmopoulos, P.G., Ningombam, S.S. and Masoom, A. Impact of aerosol and cloud on the solar energy potential over the central Gangetic Himalayan region, *Remote Sensing*, 2021, **13**, p 3248.
[26] Jiang, Y. and Yi, B. An assessment of the influences of clouds on the solar photovoltaic potential over china, *Remote Sensing*, 2023, **15**, (1), p 258.
[27] Mestnikov, N.P., Vasilyev, P.F., Davydov, G.I., Khoyutanov, A.M. and Alzakkar, A.-N. Operation of a photovoltaic installation in the North under various cloudiness conditions, *IPolytech. J.*, 2022, **26**, (1), pp 81–91.
[28] Jebar, M.A.A, Parisi, A.V., Downs, N.J. and Turner, J.F. Evaluated UVA irradiances over a twelve-year period at a sub-tropical site from ozone monitoring instrument data including the influence of cloud, *Photochem. Photobiol.*, 2018, **94**, (6), pp 1281–1288.
[29] Myers, D.R. *Solar Radiation: Practical Modeling for Renewable Energy Applications*, 2017, Boca Raton, USA: CRC press.

https://doi.org/10.1017/aer.2026.10147 Published online by Cambridge University Press

[30] Smith, C.J., Bright, J.M. and Crook, R. Cloud cover effect of clear-sky index distributions and differences between human and automatic cloud observations, *Sol. Energy*, 2017, **144**, pp 10–21.
[31] Wacker, S., Gröbner, J., Zysset, C., Diener, L., Tzoumanikas, P., Kazantzidis, A., Vuilleumier, L., Stöckli, R., Nyeki, S. and Kampfer, N. Cloud observations in Switzerland using hemispherical sky cameras, *JGR Atmospheres*, 2015, **120**, (2), pp 695–707.
[32] Kasten, F. and Czeplak, G. Solar and terrestrial radiation dependent on the amount and type of cloud, *Sol. Energy*, 1980, **24**, (2), 177–189.
[33] Wu, Z., Li, H., Roibás-Millán, E., Alonso-Moragón, A. and Jiménez-Mateos, A.G. Effect of temperature and sunlight intensity on surface of solar panels on electric power generated, *J. Phys. Conf. Ser.*, 2024, **2733**, p 012029.
[34] Duffie, J.A. and Beckman, W.A. *Solar Engineering of Thermal Processes*, Wiley, 1980, New York.
[35] Kazem, H.A. and Chaichan, M.T. Effect of environmental variables on photovoltaic performance- based on experimental studies. *Int. J. Civ. Mech. Energy Sci.*, 2016, **2**, (4), pp 1–8.
[36] Al-Luhaiby, A. Studying the effect of temperature and resistances of series (Rs) and parallel (Rsh) on the performance of the solar cell (FTO/Zn2SnO4/CdS: O/CdTe/Cu2Te) using the SCAPS-1D program, *J. Educ. Sci.*, 2022, **31**, (4), p 49.
[37] Hemond, H.F. and Fechner, E.J. *Chemical Fate and Transport in the Environment*, 2022, Academic press.
[38] Carnovale, A. and Li, X. A modeling and experimental study of capacity fade for lithium-ion batteries, *Energy AI*, 2020, **2**, p 100032.
[39] Ma, S., Jiang, M., Tao, P., Song, C., Wu, J., Wang, J., Deng, T. and Shang, W. Temperature effect and thermal impact in lithium-ion batteries: a review, *Prog. Nat. Sci.: Mater. Int.*, 2018, **28**, (6), 653–666.
[40] Song, Z., Liu, J. and Yang, H. Air pollution and soiling implications for solar photovoltaic power generation: a comprehensive review, *Appl. Energy*, 2021, **298**, 117247.
[41] Tkachyck, P., Kotcemyr, O., Sokolovskyi, S. and Bilous, D. Accounting for real meteorological conditions at the time of UAV flight mission planning, *Mil. Tech. Bull.*, 2021, **25**, pp 54–60.
[42] Chu, Y., Ho, C., Lee, Y. and Li, B. Development of a solar-powered unmanned aerial vehicle for extended flight endurance, *Drones*, 2021, **5**, (2), p 44.
[43] Dwivedi, V.S., Kumar, P., Ghosh, A.K. and Kamath, G.M. Selection of size of battery for solar powered aircraft, *IFAC-PapersOnline*, 2018, **51**, (29), pp 424–430.
[44] NASA Langley Research Center. POWER Data Access Viewer, NASA Prediction of Worldwide Energy Resources, Accessed: 16 June 2025, Available: https://power.larc.nasa.gov/data-access-viewer/
[45] Panasonic Corporation. NCR18650B Lithium-Ion Battery Specification, Accessed: 16 June 2025, Available: https://www.panasonic.com/global/about.html
[46] Linden, D. and Reddy, T.B. Handbook of batteries, *Fuel Energy Abstr.*, 1995, **4**, p 265.

Cite this article: Gencag M.S., Yildirim Dalkiran F., Kekec E.T. and Konar M. (2026). Impact analysis of solar cells on fixed-wing UAV: simulation-based performance evaluation under varying environmental conditions. *The Aeronautical Journal*, **130**, 1920–1943. https://doi.org/10.1017/aer.2026.10147

https://doi.org/10.1017/aer.2026.10147 Published online by Cambridge University Press